Application of stochastic approach to blast fragmentation modelling

I. Onederra*[1], F. Mardones[2] and C. Scherpenisse[2]

In large scale metalliferous mining, there is documented evidence that by providing an appropriate size distribution to crushing and grinding circuits, a measurable increased throughput and/or reduced power draw can be obtained. Tailoring blast designs to suit specific fragmentation requirements is becoming common place at both the prefeasibility and feasibility study stages. This is particularly the case when significant increases in ore production rates are being considered. Given the variability associated with many of the input parameters that are used to estimate fragmentation outcomes, a simple deterministic empirical approach is limited. This is the case at the feasibility stages, where there is a higher degree of uncertainty in the definition of blasting domains. Complex processes, such as explosive rock breakage and fragmentation, are suited to modelling techniques involving stochastic methods. As part of the feasibility study of a large open pit expansion project, there was a requirement to estimate fragmentation envelopes for a set of design parameters and rock mass conditions. This paper gives a description of a stochastic approach to blast fragmentation modelling and uses this expansion project to demonstrate its application. In this particular case study, there was a need to estimate the expected run of mine fragmentation associated with blasting in the deeper and more competent ore domains. Results from several simulations using the proposed modelling approach have shown the importance of including the measured variability of input parameters such intact rock properties and degree of fracturing at the feasibility stages. Modelling results also identified significant differences in ore fragmentation envelopes if current designs were to be applied in the more competent domains as the pit expands. From this analysis, a number of blast design options have been evaluated and recommendations made in order to achieve future ore handling and processing targets.

Keywords: Blasting, Open pit blasting, Fragmentation modelling, Stochastic modelling, Rock breakage

Introduction

The need to provide engineering solutions to full scale blasting problems has driven the development of several empirically based fragmentation models. Arguably, the most popular and successful models have been those applicable to surface blasting such as the Kuz–Ram model[1–4] and, more recently, the Kuznetsov–Cunningham–Ouchterlony model applying the Swebrec function.[5,6] The application of stochastic techniques using empirical methods is not a new concept. Thornton *et al.*[7] implemented a stochastic modelling technique using Monte Carlo simulations as a way of determining the most influential parameters on various fractions of the size distribution. They use a modified Kuz–Ram based empirical model and assigned a range of probability density functions to a selection of input parameters including blasthole pattern geometry, explosive performance parameters and rock mass parameters. From this analysis, the advantages of adopting a stochastic approach to consider the inherent variability of rock mass parameters were clearly demonstrated.

Blasting activities in major mining operations have been placing significant emphasis on the ability to tailor fragmentation to improve downstream processes. At the conceptual and feasibility stages, fragmentation modelling studies, which support future mine to mill strategies, can be conducted through the calibration of empirical models using existing data and, if need be, through the implementation of specific trials. As part of the feasibility study of a large open pit expansion project, the authors were asked to calibrate and apply a stochastic modelling technique to estimate run of mine (ROM) fragmentation in both current and deeper ore domains. As will be discussed in this paper, the proposed

[1]The University of Queensland, Sustainable Minerals Institute, W H Bryan Mining and Geology Research Centre, Brisbane, Qld, Australia
[2]GeoBlast S. A., Santiago, Chile

*Corresponding author, email i.onederra@uq.edu.au

Published by Maney on behalf of the Institute and The AusIMM
Received 8 June 2010; accepted 4 October 2010
DOI 10.1179/1743286310Y.0000000003

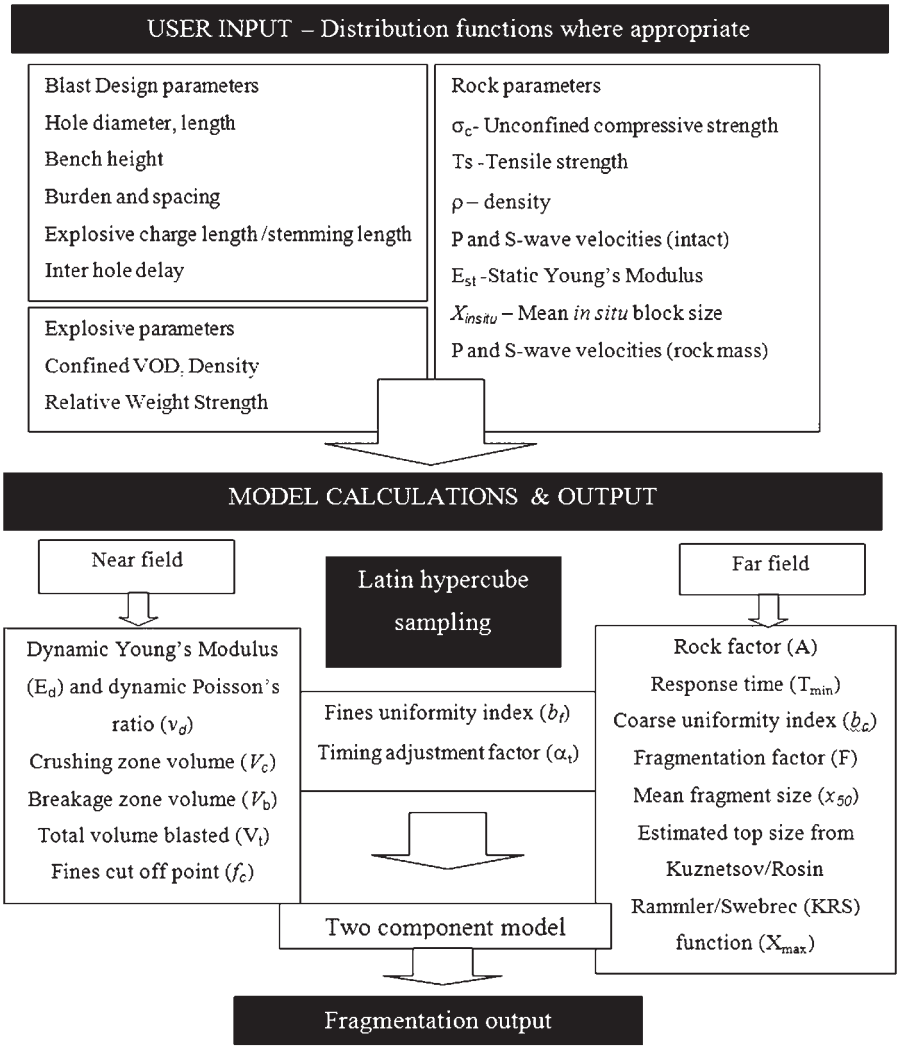

1 Blast fragmentation modelling framework

stochastic technique builds upon work previously conducted in blast fragmentation modelling. The approach provides an improved modelling framework, which includes the use of the Swebrec function,[5] an improved crushed zone model[8] and timing correction factors to consider the observed influence of interhole delay on fragmentation.[9]

Proposed fragmentation model

As shown in Fig. 1, the modelling framework includes the ability to consider a range of values to key input parameters through the explicit definition of distribution functions. In this way, stochastic simulations can be conducted to determine fragmentation envelopes that take into account the variability of rock material, rock mass, blast geometry and explosive performance parameters. In general, the expected distribution of fragments in the fine and coarse regions is modelled by two separate distributions based on the Swebrec function.[5] The Swebrec function has recently shown to be far superior in fitting fragmented rock in the intermediate and finer end of the fragmentation curve than previous models. In the coarse end, the shape of the distribution is very similar to the widely used Rosin–Rammler function. The framework is currently implemented in a excel spreadsheet format and uses the @RISK software package from the Palisade Corporation (Ithaca, NY, USA). Simulations are run using the Latin hypercube sampling technique where samples are generated from all the ranges of possible values, thus giving better insight into the extremes of the probability distributions of the outputs. One of the advantages of the Latin hypercube sampling technique is that it helps recreate the input distributions through sampling in fewer iterations when compared with the Monte Carlo technique. It is beyond the scope of this paper to describe in detail all of the key components of the proposed framework; however, the key empirical relationships are discussed within this section with further details referred to in other publications.

Adopted fragmentation size distribution functions

The form of the fragmentation size distribution functions adopted in the modelling approach are based on the Swebrec functions proposed by Ouchterlony[5] and given by

$$R(x) = \frac{1}{1 + \left[\frac{\ln\left(\frac{X_{\max}}{x}\right)}{\ln\left(\frac{X_{\max}}{X_{50}^{t}}\right)}\right]^{b_{fines}^{t}}} \quad \text{for values of } x \le X_{50}^{t} \quad (1)$$

$$R(x) = \frac{1}{1 + \left[\dfrac{\ln\left(\dfrac{X_{max}}{x}\right)}{\ln\left(\dfrac{X_{max}}{X_{50}^{t}}\right)}\right]^{b_{coarse}^{t}}} \quad \text{for values of } x \geq X_{50}^{t} \quad (2)$$

where $R(x)$ is the proportion of the material passing a screen of size x. X_{50}^{t}, b_{fines}^{t} and b_{coarse}^{t} are the corrected mean fragment size and uniformity parameters given by

$$b_{coarse}^{t} = \left[2 \times \ln(2) \times \ln\left(\frac{X_{max}}{X_{50}^{t}}\right)\right] n_{coarse} \quad (3)$$

$$b_{fine}^{t} = \frac{\ln\left[\left(\dfrac{1}{f_c^{t}}\right) - 1\right]}{\ln\left[\dfrac{\ln\left(\dfrac{X_{max}}{x_f}\right)}{\ln\left(\dfrac{X_{max}}{X_{50}^{t}}\right)}\right]} \quad (4)$$

where n_{coarse} is the base case or uniformity index calculated from relationships based on single hole firing conditions such as those proposed by Cunningham[4] and/or Onederra and Riihioja.[10] It should be noted that x_f (equation (4)) refers to the fine top size value, which is assumed to be 1 mm, and α_t (in equation (5)) is the interhole delay timing factor defined by the following criteria

$$\alpha_t = \left(1 - \frac{dt}{T_{min}}\right) \text{ for } dt/T_{min} < 1 \quad (5)$$

or

$$\alpha_t = 0 \text{ for } dt/T_{min} \geq 1 \quad (6)$$

Minimum response time T_{min} is here defined as a discrete element of time, which elapses from the time of explosive detonation to mass burden displacement, and can be estimated by the approach discussed in more detail by Onederra.[11] In equation (6), dt is the interhole delay time, and from the above expression, dt/T_{min} ratios ≥ 1 correspond to the single hole firing case or where no cooperation between charges is expected. The theoretical basis of this correction factor can also be associated with the period of time in which both stresses and gasses are likely to act on the rock mass to generate fractures and thus influence fragmentation. This time is bound by the detonation of the explosive charge, the propagation and interaction of stresses and the work done by gasses before rock mass detachment.

X_{max} is the expected top size. A simple approach is used to define this parameter in the proposed modelling approach. It is based on the application of a Rosin–Rammler distribution at the coarse end of the expected fragment size distribution; the top size or X_{max} value is estimated at the 99% passing fraction.

X_{50}^{t} is the corrected mean fragment size, and f_c^{t} is the corrected proportion of fines. These parameters are discussed in the following section.

Estimation of mean fragment size

The expected mean fragment size predicted by conventional formulae (e.g. Kuznetsov[1] and Cunningham[3]) and referring to the base case of single hole firing conditions is corrected with the following relationships

$$X_{50}^{t} = \frac{X_{in\ situ}}{1 + F^{t}} \quad (7)$$

$$F^{t} = F(1 + \alpha_t) \quad (8)$$

$$F = \frac{X_{in\ situ}}{X_{50}} - 1 \quad (9)$$

where X_{50}^{t} is the corrected mean fragment size, F^{t} is the corrected fragmentation efficiency factor, F is the base case fragmentation efficiency factor, $X_{in\ situ}$ is the mean *in situ* block size and X_{50} is the base case predicted post-blast mean fragment size using conventional formulae (e.g. Cunningham[4]). As described, the base case fragmentation efficiency factor F (i.e. single hole firing conditions) is hypothesised to increase when there is evidence of positive interaction (cooperation) between blastholes. This will cause an increase in the proportion of intermediate and fine fragments, as has been shown in the literature.[12] It should be mentioned that the fragmentation efficiency factor F discussed above was first introduced and discussed by Onederra[13] as part of an alternative approach to predict mean fragment size in underground ring blasting conditions.

The interhole delay timing factor α_t is defined by the following criteria.

Estimation of proportion of fines

Following a two-component modelling approach, the proportion of fines generated by blasting given by the fines parameter f_c (*see* Onederra *et al.*[8]) is corrected with the following expression

$$f_c^{t} = f_c\left(1 + \frac{\alpha_t}{3}\right) \quad (10)$$

where f_c is the proportion of the material passing a screen of size 1 mm or the fine inflection point estimated with the crushed zone and fracturing model discussed by Onederra *et al.*[8] Literature indicates that fines present in a muckpile tend to originate from the near field crushing zone, fracturing (shearing) zones as well as possible liberation from rock mass discontinuities.[12,14,15] The fine inflection point is introduced to consider these sources and is given by

$$f_c = \%\text{fines}_{(-1\,mm)}\left(\frac{V_c + V_b}{V_t}\right) \times 100 + [F_r] \quad (11)$$

where V_c is the volume contribution of the crushed zone, V_b is the volume contribution from breakage (major radial cracks), V_t is the total volume being blasted and F_r is a rock mass fines correction factor.

The fine inflection point is based on the hypothesis that, for most conditions, the coarsest particle size expected to be generated during the crushing and shearing stages of blasting would be 1 mm and that the per cent passing fraction would be directly proportional to the volume of crushed and/or sheared rock material surrounding a detonated blasthole.

The estimation of the volume of crushed and/or sheared rock material follows simple geometric calculations given by the radius of crushing, and thus the volume of a cylinder of crushed rock, and the distribution of major radial cracks, which are assumed to be evenly distributed around a borehole, planar and also continuous along the length of the explosive charge.

These two components define the total volume of a 'star' shaped crushed region.

In the proposed relationship, a rock mass correction factor F_r has been introduced to address the hypothesis that fines may also be liberated from rock mass discontinuities.[14] However, an approach to determine this parameter has not been developed, as there is insufficient quantifiable evidence to support this. To simplify the modelling structure, the F_r parameter is therefore currently disregarded, and the modelling process involves only the determination of V_c and V_b, which is described below.

Crushed zone model to determine V_c

The determination of V_c is based on an improved model to predict the radius of crushing generated by a detonated blasthole reported by Esen *et al.*[15] This model is given by the following empirical relation

$$r_c = 0{\cdot}812 r_o (CZI)^{0{\cdot}219} \tag{12}$$

where r_c is the crushing zone radius (mm), r_o is the borehole radius (mm) and CZI is defined as the crushing zone index. This is a dimensionless index that identifies the crushing potential of a charged blasthole and is calculated by

$$CZI = \frac{(P_b)^3}{(K) \times \sigma_c^2} \tag{13}$$

where P_b is the borehole pressure (Pa), computed from non-ideal detonation theory, K is the rock stiffness (Pa) and σ_c is the uniaxial compressive strength (Pa). Rock stiffness K is defined assuming that the material within the crushing zone is homogeneous and isotropic and is given by

$$K = \frac{E_d}{1 + \upsilon_d} \tag{14}$$

where E_d is the dynamic Young's modulus (Pa) and v_d is the dynamic Poisson's ratio.

As discussed by Esen *et al.*,[15] this model has been shown to have better predictive capabilities than other documented approaches. Its validity has also been confirmed with data obtained from full scale blasting conditions.

Crack model to determine V_b

The following approach assumes that the source of fines from overall breakage is directly proportional to a volume of crushed material bounded by major blast induced fractures. The number of near field radial cracks C around the blasthole is estimated following the approach proposed by Katsabanis[16]

$$C = \varepsilon_s \left(\frac{P_b}{T_d} \right) \tag{15}$$

where ε_s is the strain at the blasthole and T_d is the dynamic tensile strength of the rock (Pa), which is assumed to be in the range of 4–8 times the static value.

The strain at the blasthole wall ε_s can be approximated by Katsabanis[16]

$$\varepsilon_s = \frac{(1-\upsilon) P_b}{2(1-2\upsilon)\rho v_p^2 + 3(1-\upsilon)\gamma P_b} \tag{16}$$

where P_b is the explosion or borehole pressure (Pa), ρ is the rock density (kg m^{-3}), v_p is the P wave velocity (m s^{-1}), γ is the adiabatic exponent of the detonation products and υ is the Poisson's ratio of the rock.

The length or radial extension of cracks C_l is determined empirically with a stress attenuation function similar to that proposed by Liu and Katsabanis,[17] assuming that the crack will arrest when the induced stress is equal to the static tensile strength or the rock material. In this case, the following relationship is used

$$C_l = r_o \left(\frac{T_s}{P_{eq}} \right)^{1/\varphi} - r_c \tag{17}$$

where T_s is the static tensile strength of the rock (Pa), r_o is the blasthole radius (m), r_c is the radius of crushing (m), ϕ is the pressure decay factor and P_{eq} is the equilibrium pressure (Pa) or the pressure experienced at the end of the crushing zone, which is given by

$$P_{eq} = P_b \left(\frac{r_c}{r_o} \right)^{\varphi} \tag{18}$$

The pressure decay factor ϕ is a function of rock and explosive properties. It is a negative number that has

Table 1 Summary of intact rock properties in secondary and primary rock mass domains*

Domain and rock types		Secondary		Primary	
ID		S-G	S-B	P-G	P-B
ρ, g cc^{-1}	Mean	2·659	2·724	2·679	2·759
	SD	0·062	0·096	0·053	0·060
V_p, m s^{-1}	Mean	4719	4582	4577	4767
	SD	843	699	386	373
V_s, m s^{-1}	Mean	2841	2680	2903	2961
	SD	313	315	362	230
Unconfined compressive strength, MPa	Mean	161	135	156	158
	SD	41	35	34	46
T_s, MPa	Mean	10·2	11·8	12·5	12·6
	SD	2·4	4·2	2·6	3·2
E, GPa	Mean	51	49	57	66
	SD	12	12	13	23
V	Mean	0·26	0·25	0·25	0·27
	SD	0·04	0·03	0·06	0·07

*S-G: secondary granodiorite; S-B: secondary breccia; P-G: primary granodiorite; P-B: primary breccia.

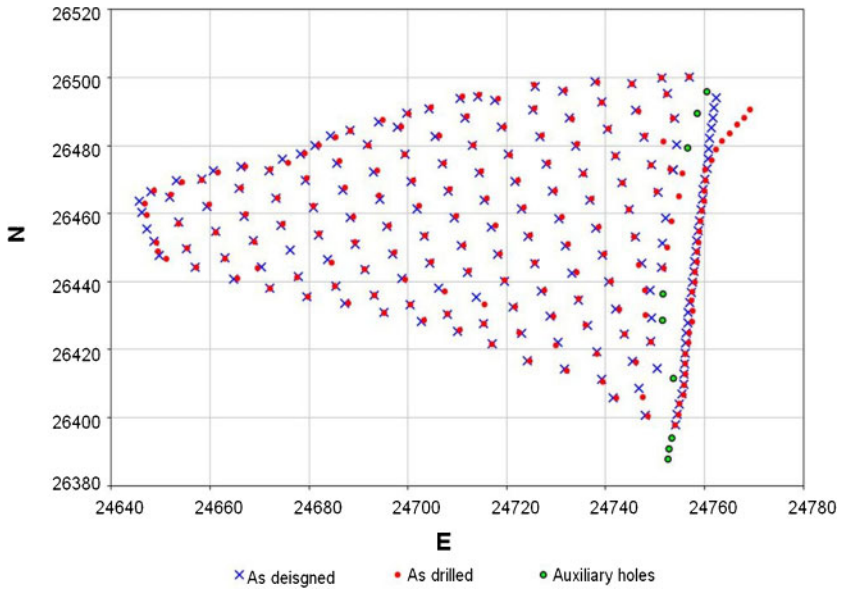

2 Drilling compliance of blast 3724_12

been found to be in the range of −1·24 to −1·65 for a wide range of explosive and rock combinations.[17,18]

Data collection and model calibration

A large open pit operation undergoing a significant expansion was part of the case study in which the proposed stochastic fragmentation model was applied. In this operation, blasting domains were mainly associated with what is referred to as secondary and primary rock masses. In both cases, the major rock types included Granodiorites (G) and Breccias (B). The physical properties of the intact rock types in these two domains are summarised in Table 1. Primary rock masses can be described as 'hard' with well healed gypsum or anhydrite filled fractures, typical resting metabolic rate values are in the range of 60–80. Primary rock masses are found in the deeper part of the deposit and correspond to future ore reserves. Secondary rock masses are part of the current blasting schedule and can also be described as 'hard'; however, fractures are generally open and hence reduce the competency of the rock mass with characteristic resting metabolic rate values in the range of 42–50.

Relevant to blast fragmentation modelling, and particularly in the definition of input parameters, such as X_{max} or $X_{in\ situ}$, is the degree of *in situ* fracturing. Total spacing statistics derived from fracture frequency data at this site showed that the degree of fracturing is more intense in the secondary rock mass domains. Results from the available core logging data indicated that total fracture spacing may be as wide as 0·4 m in the secondary domain and 0·91 m in the primary rock domain. The analysis also indicated that the variability in fracture intensity appears to be greater in the primary rock domain. From a drilling and blasting perspective, the secondary and primary domains can be classified as fractured and blocky rock masses respectively.

Monitored blasts for calibration purposes

As summarised in Table 2, four production blasts were monitored in secondary rock masses to calibrate the proposed modelling framework, three were located in the secondary granodiorite (S-G) domain and one in the secondary breccia (S-B) domain.

As illustrated in Fig. 2, direct measurements taken during the implementation of the monitored blasts confirmed that the difference between 'as designed' and 'as drilled' conditions was within acceptable limits. Analysis indicated that large discrepancies (>1 m) between as designed and as drilled blastholes were only observed at the blast boundaries where operational conditions require specific changes to the pattern

Table 2 Design parameters of monitored production blasts

Blast ID	3724-10	3724-12	3724-09	3708-03
Blast type	Production	Production	Trim	Production
Domain	S-G	S-G	S-G	S-B
Bench height, m	16	16	16	16
Blasthole diameter, mm	270	270	270	270
Burden, m	6	7	6	6
Spacing, m	7	8	7	7
Interhole delay, ms	2	2	2	2
Number of blastholes	267	193	182	183
Tonnes blasted	422 385	355 493	263 428	318 956
Explosive type	Heavy ANFO	Heavy ANFO	Heavy ANFO	Heavy ANFO
Explosive density	1·32	1·32	1·32	1·32
Blasthole length, m	17	17	17	17
Charge length, m	10·5	11	10·5	10·5
Stemming length, m	6·5	6	6·5	6·5
Actual powder factor, g t^{-1}	432	348	419	332

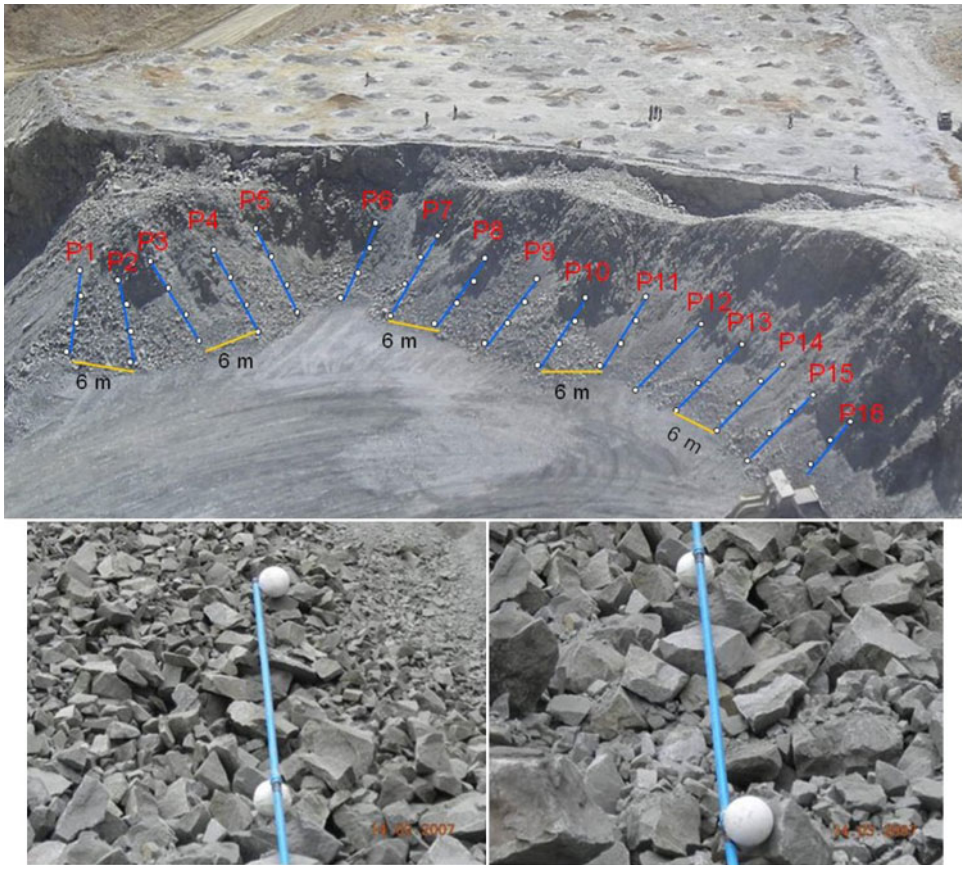

3 Example plan view of sampling lines of blast 3724_12

geometry (e.g. presplit layout). The potential impact on fragmentation given by variations in spacings, and burdens are further discussed in the application of the stochastic model in the primary ore zones.

With regard to explosive performance, velocity of detonation monitoring conducted during the study showed that the main explosive product achieved values of ~4600 m s^{-1} in 270 mm diameter holes. For model calibration and verification purposes, a normal distribution was assumed with a mean value of 4500 m s^{-1} and a standard deviation of 200 m s^{-1}.

Fragmentation assessment

A detailed fragmentation assessment programme was conducted during this study. The programme included the acquisition of images during the excavation of muckpiles as well as the sieving of a limited number of samples taken from selected regions to calibrate the image analysis software. The assessment procedure consisted of sampling lines and images taken at different stages of extraction in each sampling line. Figure 3 illustrates the type of images taken for one sampling line. The total number of samples taken in the secondary rock mass is summarised in Table 3. This procedure was consistent with best practices in fragmentation assessment using image analysis methods in large scale operations.

Detailed fragmentation analysis included both manual editing and the definition of site specific fine correction factors. These factors were determined directly by the sampling and sieving of fragments in the areas of interest. Blasting literature[19,20] shows that reliable estimates of ROM fragmentation can be obtained following procedures similar to those incorporated in this study.

Calibration procedure and results

The calibration procedure adopted in this study consisted of the following.

First, on a domain by domain basis, conduct first pass modelling of ROM fragmentation envelopes using the design and rock mass data available from all monitored blasts.

Second, determine the differences between measured and predicted values in the fines, intermediate and coarse regions. Calibration parameters are applied to

Table 3 Summary of fragmentation images samples taken during monitoring of blasts in secondary rock masses (S-G and S-B domains)

Blast ID	3724-10	3724-12	3724-09	3708-03
Blast type	Production	Production	Trim	Production
Domain	S-G	S-G	S-G	S-B
Number of sampling lines	3	4	5	3
Number of profiles	46	41	24	35
Samples per profile	3	3	3	3
Total number of samples	138	123	72	105

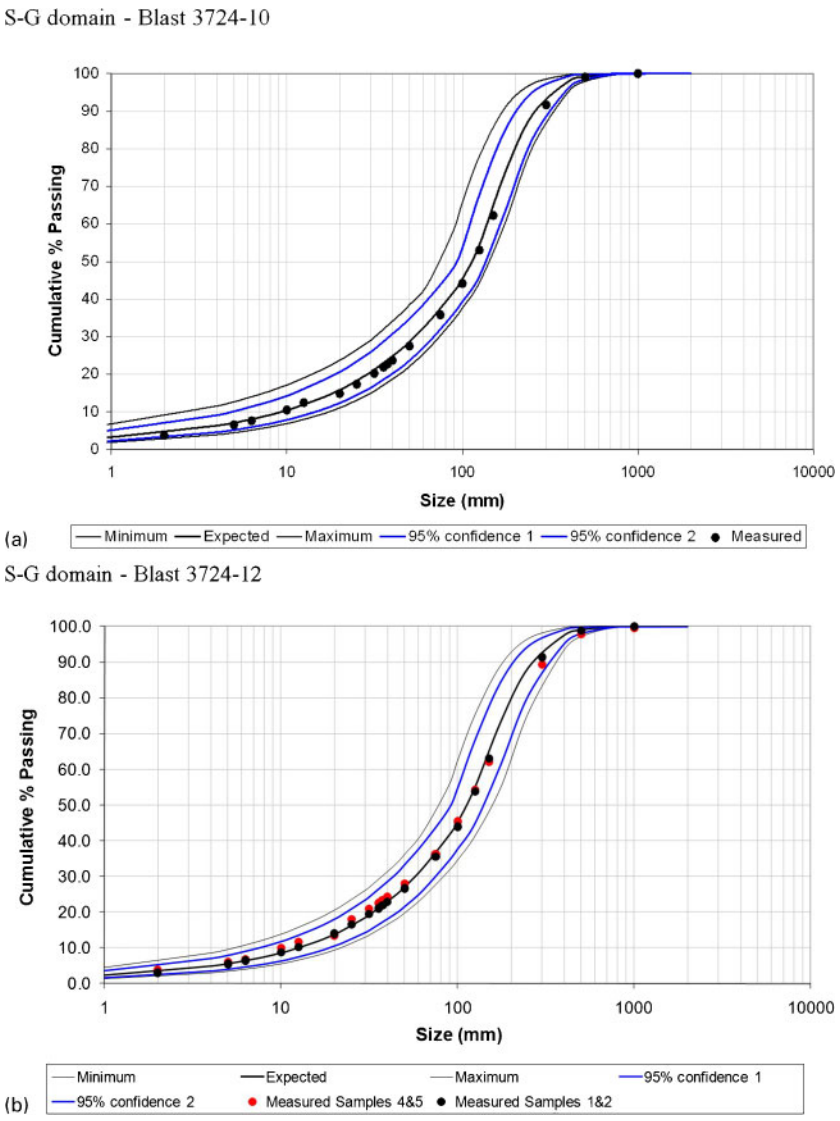

4 Example of calibration results from blast 3724-10 and 3724_12

fragmentation uniformity parameters and the estimation of the mean fragment size. The main criteria involved minimising the differences in the 20, 50 and 80% passing fractions. A calibrated model would be accepted when these differences are minimised, and the measured data are within the predicted 95% confidence envelopes.

The need for model calibration is associated with the degree of uncertainty attached to rock mass input parameters such as the mean size of *in situ* blocks, the orientation and characteristics of discontinuities and their potential impact on the uniformity of fragmentation, as well as the propensity of the rock fabric to generate or liberate fines within discontinuities, a phenomenon that is sometimes referred to as the liberation of *in situ* fines.

Three parameters are used in the model calibration procedure (i.e. *A*, *B* and *C*), and these are described in Table 4 below. Note that depending on preliminary modelling results, not all parameters may need to be modified in order to calibrate the domain specific model. In the cases described in Table 4, calibration parameters can be easily determined graphically by matching changes in the predicted fragmentation curve against the superimposed measured data. The range of calibration parameters values is of the order of 0·5–1·5. As expected, a value of 1·0 indicates that no change is

Table 4 Domain specific calibration parameters

Modelling component	Description
$X_{50}^{t} = \frac{(X_{\text{in situ}})A}{1+F^{t}}$	When the measured mean fragment size is less than the predicted value, A<1; when the measured mean fragment size is greater than the predicted value, A>1
$b_{\text{coarse}}^{t} = \left[(2B) \times \ln(2) \times \ln\left(\frac{X_{\max}}{X_{50}^{t}}\right)\right] n_{\text{coarse}}$	When the measured fragmentation is more uniform than predicted, B>1; when the measured fragmentation is less uniform than predicted, B<1
$b_{\text{fines}}^{t} = (b_{\text{fines}}^{t})C$	When the amount of fines measured is less than predicted, C>1; when the amount of fines measured is more than predicted, C<1

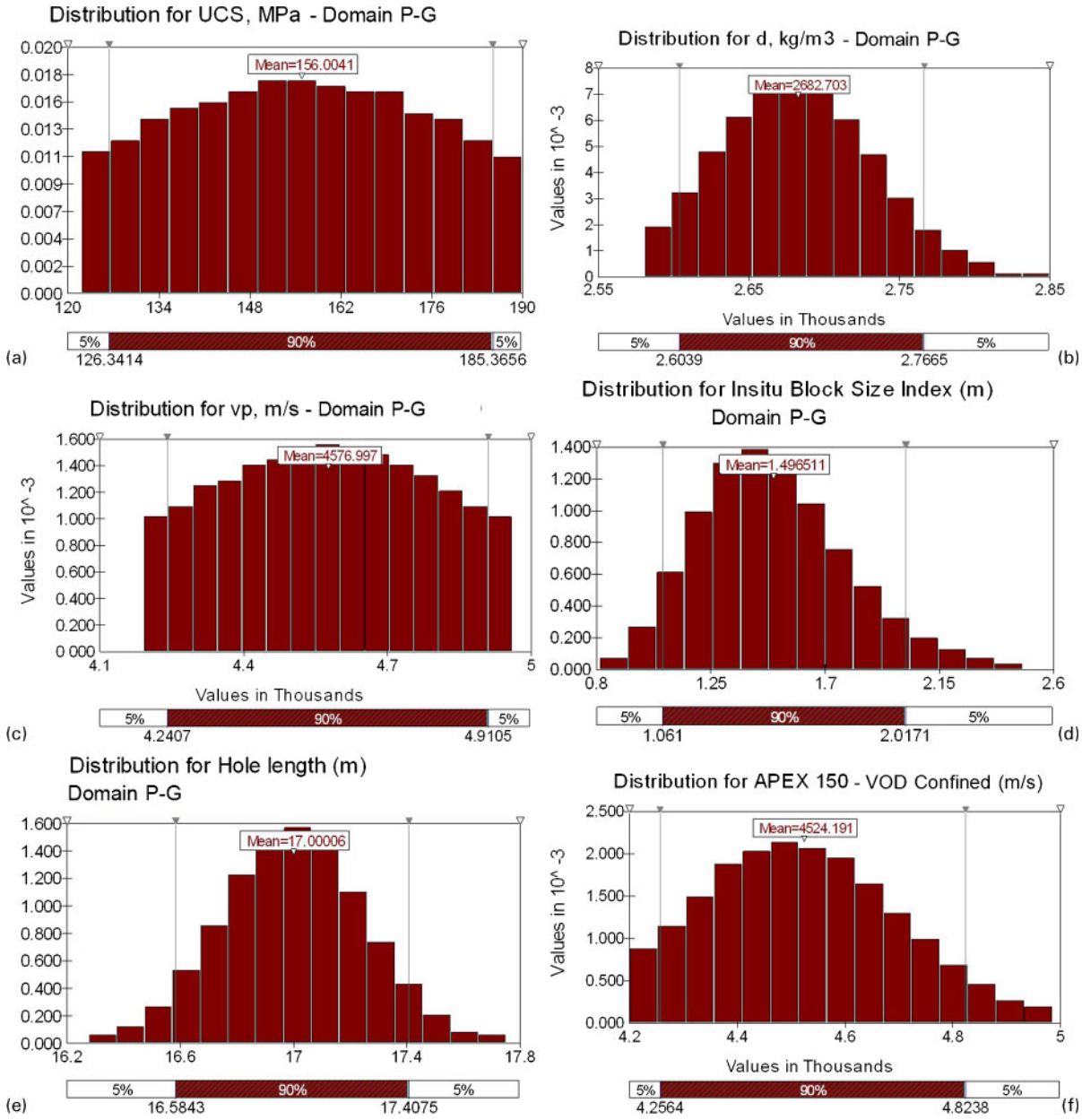

5 Example of input parameter distributions for simulation no. 2, design D2

Table 5 Summary of pattern configurations for P-G and P-B primary ore domains

Simulation no.	Design ID	Burden, m	Spacing, m	Stemming, m	Explosive type*	Domain	Theoretical powder factor, kg t^{-1}
1	D1	7	8	5	HA150	P-G	0·37
2	D2	6	7	5	HA150	P-G	0·50
3	D3	5	6	5	HA150	P-G	0·69
4	D4	7	8	5	HA165	P-G	0·34
5	D5	6	7	5	HA165	P-G	0·46
6	D6	5	6	5	HA165	P-G	0·64
7	D7	7	8	5	HA150	P-B	0·36
8	D8	6	7	5	HA150	P-B	0·48
9	D9	5	6	5	HA150	P-B	0·67
10	D10	7	8	5	HA165	P-B	0·33
11	D11	6	7	5	HA165	P-B	0·44
12	D12	5	6	5	HA165	P-B	0·62
13	D2A	6	7	4	HA150	P-G	0·54
14	D8A	6	7	4	HA150	P-B	0·52

*HA150 and HA165 are heavy ANFOs with 50 and 65% emulsion respectively.

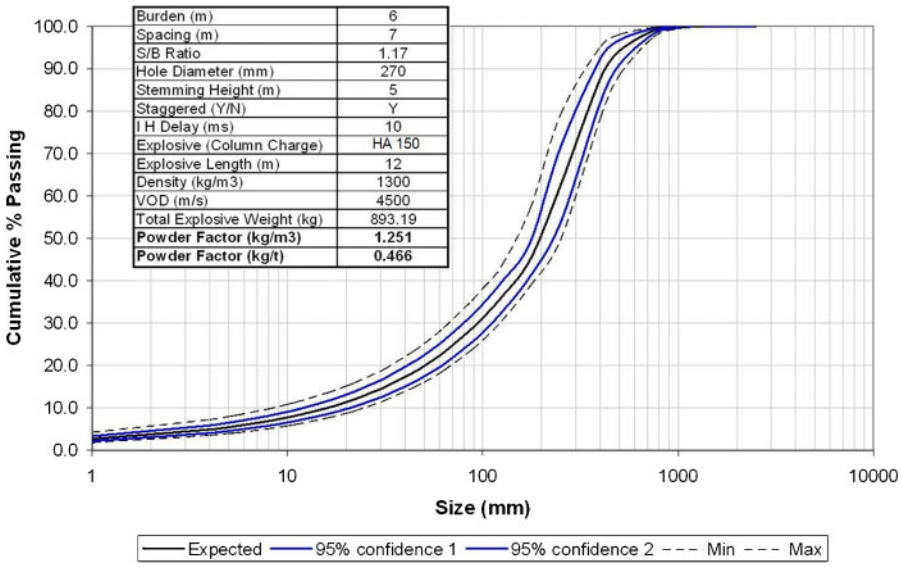

6 Example ROM fragmentation output for simulation D2

required in order to match first pass predictions with measured data.

Figure 4 gives an example of the final results of the calibrated model in the S-G domain using data from the production blasts 3724-10 and 3724-12. It should be noted that data from the trim blast 3724-09 were also used in the calibration process. In this analysis, statistics associated with rock material input parameters, pattern geometry and explosive performance was included to generate an expected fragmentation bounded by envelopes of minimum, maximum and 95% confidence limits. As shown in Fig. 4, measured data were closely matched to the expected ROM fragmentation, and the calibration parameters for the S-G domain were determined to be $A=0{\cdot}9$, $B=1{\cdot}25$ and $C=1{\cdot}13$. The relatively close matching provided a higher degree of confidence in the original rock mass input parameters (e.g. fracture frequency data) derived from the available core data. The same calibration approach was carried out for the S-B domain using blast 3708-03.

Fragmentation modelling of production blasts in primary ore

The application of the proposed stochastic modelling approach was subject to the following assumptions.

First, pattern geometries were expected to achieve full breakage within the volume defined by the spacing, burden and bench height.

Second, no variation in drilling layout geometry was accounted for in this study; that is, burden and spacings were assumed to be consistent throughout the pattern. Variation was only accounted for in blasthole lengths.

Third, block size indices describing the degree of fracturing of different domains can be determined from core data. These indices were further refined through the model calibration (back analysis) process in secondary ore blasting. The calibration parameters were kept constant for subsequent modelling in primary ore domains, considering that the main differences between the two domains were only associated with changes in fracture frequency.

Fourth, rock material and rock mass variability can be modelled with the introduction of explicit distribution functions. These input functions are defined by the mean, standard deviation and minimum and maximum values associated with each parameter.

Fifth, variability in explosive performance was modelled by a range of velocity of detonation values normally distributed about the mean.

Sixth, stemming lengths were assumed to provide the necessary energy confinement to achieve complete breakage.

Seventh, interhole delays of less than the expected burden response time were assumed to contribute to hole interaction and therefore improve potential fragmentation outcomes. Inter-row delays were assumed to provide optimum burden relief.

A total of 14 simulations were conducted to quantify relative changes in ROM fragmentation in primary rock. Table 5 gives a summary of the pattern geometries and powder factor ranges investigated. The design parameters reflected the use of pattern geometries similar to those currently used at the operation, as well as more aggressive designs, which include both reductions in burden, spacing and stemming lengths. All simulations have maintained the use of 270 mm diameter blastholes using HA150 and HA165 as the base case explosive products. It should also be noted that a single hole firing mode was assumed with interhole delays of 10 ms.

As discussed earlier, the adopted stochastic approach has allowed the inclusion of distribution functions to rock material and rock mass input parameters as well as design specific parameters, such as hole and charge lengths. The Latin hypercube sampling technique was used with simulations set to 500 iterations. An example of the input parameter functions used in a given scenario is shown in Fig. 5. As shown, the majority of input parameters were modelled with truncated normal and log normal distributions based on the mean, standard deviation, minimum and maximum values available.

Overall results and discussion

An example of the ROM fragmentation output from one design scenario (e.g. D2) is shown in Fig. 6. Fragmentation modelling results for P-G and P-B primary ore domains are summarised in Figs. 7 and 8

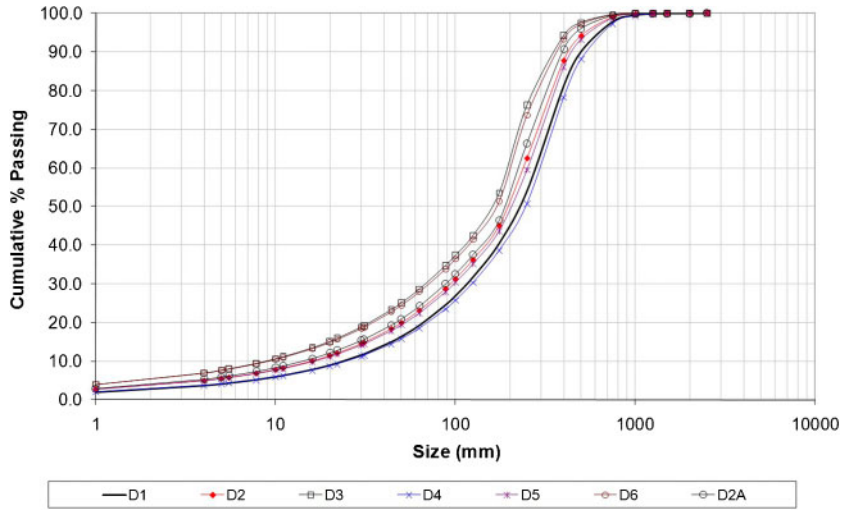

7 Comparison between designs in P-G primary ore domain

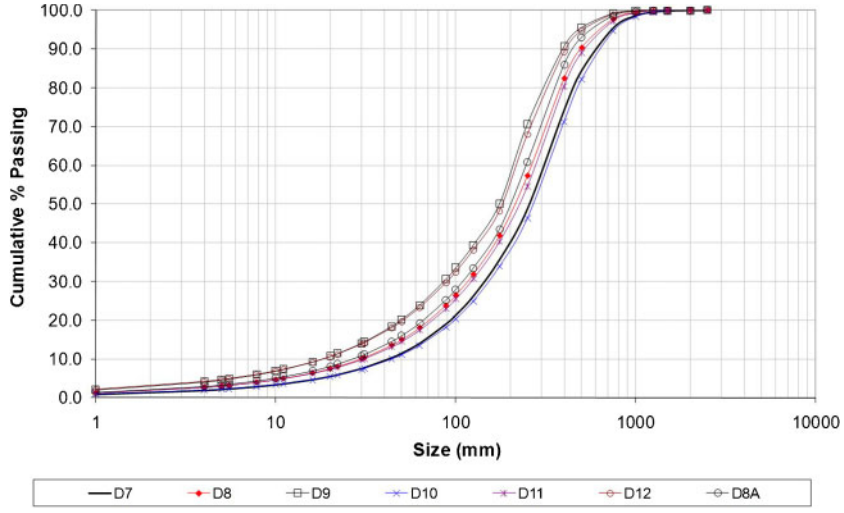

8 Comparison between designs in P-B primary ore domain

respectively. Note that only the expected size distribution curves are shown here for comparison purposes. Modelling results demonstrate the influence that changes in pattern geometry may have on fragmentation, particularly in the intermediate and finer size fractions. Differences between domains and designs have also been summarised in Table 6.

For similar pattern geometries and corresponding powder factors, modelling results suggest that blasting in the P-G domain has the potential to generate more fines

Table 6 Summary of fragmentation modelling results in primary ore conditions*

Blasting domain	Design ID	% Passing ½″ (12·7 mm)	% Passing 1″ (25·4 mm)	% Passing 1½″ (38 mm)	B, m	S, m	Stemming, m	Explosive	Theoretical powder factor, kg t^{-1}
P-G	D1	7·0	10·5	13·5	7	8	5	HA150	0·37
	D2	8·7	13	16·5	6	7	5	HA150	0·50
	D3	12	17·2	21	5	6	5	HA150	0·69
	D4	7·0	10	13	7	8	5	HA165	0·34
	D5	8·7	12·8	16	6	7	5	HA165	0·46
	D6	11·8	17	20·5	5	6	5	HA165	0·64
	D2A	9·5	14	17·5	6	7	4	HA150	0·54
P-B	D7	4·0	6·7	9·2	7	8	5	HA150	0·36
	D8	5·5	9·0	12·2	6	7	5	HA150	0·48
	D9	8·0	12·6	16·5	5	6	5	HA150	0·67
	D10	4·0	6·5	8·9	7	8	5	HA165	0·33
	D11	5·5	8·8	11·9	6	7	5	HA165	0·44
	D12	8·0	12·2	16·2	5	6	5	HA165	0·62
	D8A	6·0	9·5	13	6	7	4	HA150	0·52

*HA150 and HA165 are heavy ANFOs with 50 and 65% emulsion respectively.

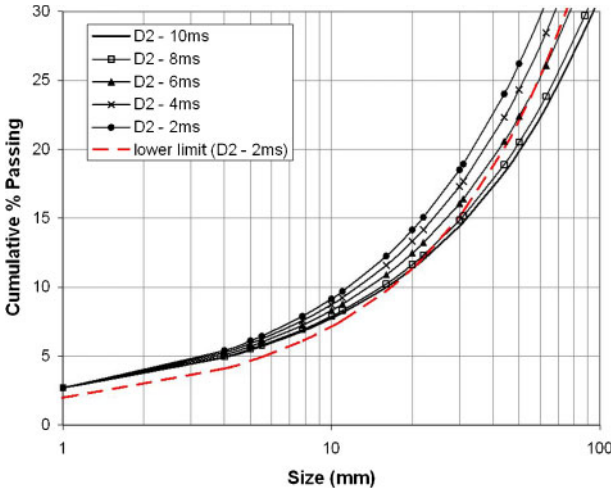

9 Modelling results showing potential influence of short interhole delay times on fragmentation outcomes for design D2 (P-G domain)

than in the P-B domain. Relative differences may be of the order of 3–5% between these two domains. As expected, designs D3 and D6 give the finest fragmentation in the P-G domain, and designs D9 and D12 give the finest fragmentation in the P-B domain. By comparing designs D2 and D2A, modelling results suggest that by decreasing stemming lengths by ~1 m, a 1% gain is expected in the amount of fines generated in the P-G domain. In the P-B domain, however, the gain is only ~0·5%, as shown by comparing designs D8 and D8A.

As discussed earlier, single hole firing conditions were adopted in the modelling calculations; in this case, a 10 ms inter hole delay was assumed based on estimations of minimum response time.[11] The current modelling framework was used to investigate potential gains in fines generation by introducing shorter delays (e.g. 2–10 ms). Design D2 was used as a base case for the P-G domain. Results of the analysis for the expected values in P-G are summarised in Fig. 9. As shown, for the ½″ (12·7 mm) and 1″ (25 mm) size fractions with the use of interhole delays of 2 ms, gains of approximately 2 and 3·5% may be achieved in the P-G. The use of very short inter hole delays (e.g. 2 ms) demonstrates gains in the intermediate and fine fractions; however, as shown in Fig. 8, these gains may not be significant if one is to consider the variation associated with modelling predictions and, in particular, the lower limit predictive envelope. It should also be noted that the interhole delay adjustment factors proposed in the current modelling framework[9] are based on limited data, and further validation work will still be required in primary ore conditions.

Although fragmentation may be improved, it is important to note that 'high intensity' blasting with the use of short interhole delays (e.g. 2 ms) may be counterproductive if the risk of rock mass damage is increased and loading productivity is influenced by the lack of muckpile looseness. Preliminary modelling results have highlighted the need to further quantify the potential impact of short delays on near field damage and downstream loading productivity. This should be considered a priority if short interhole delays were to be used in primary ore production blasting.

It is important to note that simulations are indicative of what may be achieved if all measured and assumed modelling conditions are met. Actual measurable results will undoubtedly be influenced by the field implementation process. For this reason, the implementation of a quality assurance/quality control strategy was recommended, particularly as improved designs are implemented in both current and future domains (secondary and primary rock domains). To emphasise this point, the impact on fragmentation outcomes given by variations in pattern geometry was demonstrated for design D2 and is shown in Fig. 10. In this case, a standard deviation of 0·5 m was assumed for the mean values of burden and spacing. Results show a widening of the predictive envelope, which can translate into coarser or more bimodal fragmentation outcomes. The analysis shows that systematic variations in Burden and Spacings are likely to impact on fragmentation outcomes. The main limitations of the current approach is that the assumed variations are assigned to the whole blasting area, while measured data suggest that drilling errors can be associated with specific operational constraints in specific areas of a blast.

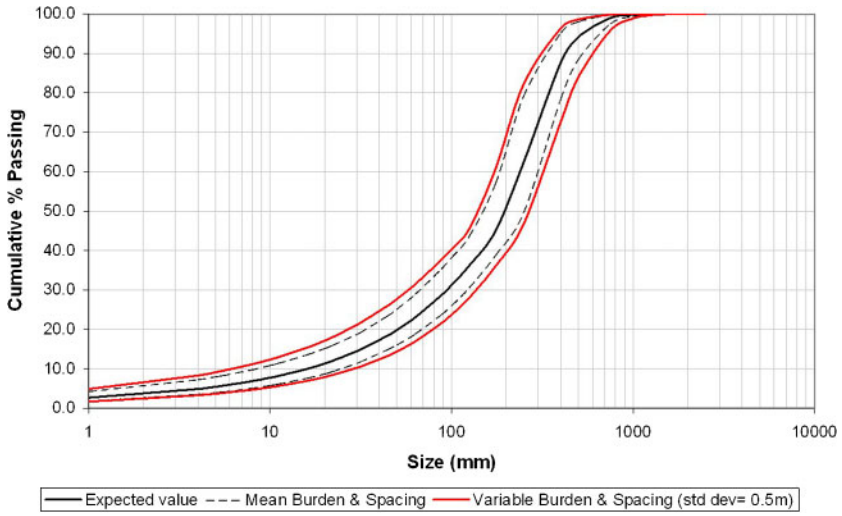

10 Potential impact on fragmentation outcomes given by simulated variations in pattern geometry

Conclusions

The objective of this paper was to demonstrate the potential application of stochastic techniques in blast fragmentation modelling. A case study was used to calibrate and apply the proposed modelling framework. A total of four production blasts were comprehensively monitored to calibrate the model; three were located in the S-G domain and one in the S-B domain. The calibration process allowed the definition and refinement of estimates associated with key rock mass indices, which impact on the expected uniformity, mean fragment size and the propensity of the rock fabric to generate fines.

The proposed model was applied by running 14 design simulations in the future primary rock domains (i.e. P-G and P-B domains). These simulations allowed a quantification of the relative changes in ROM fragmentation outcomes in primary rock. The following can be concluded from the range of pattern geometries and corresponding powder factors.

1. For similar pattern geometries, blasting in the P-G domain would have the potential to generate more fines than in the P-B domain. Relative differences may be of the order of 3–5% between these two domains.

2. Designs D3 and D6 give the finest fragmentation in the P-G domain, and designs D9 and D12 give the finest fragmentation in the P-B domain. By comparing designs D2 and D2A, modelling results suggested that by decreasing stemming lengths by ~1 m, a 1% gain is expected in the amount of fines generated in the P-G domain. In the P-B domain, however, the gain was only ~0·5%, as shown by comparing designs D8 and D8A. Designs D2 and D5 for P-G and designs D9 and D12 for P-B are expected to yield similar ROM fragmentation outcomes.

3. The calibrated modelling framework was also used to investigate potential gains in fines generation by introducing shorter interhole delays. Design D2 was used as a base case for the P-G domain. Results from this preliminary analysis indicated that for the ½″ (12·7 mm) and 1″ (25·4 mm) size fractions with the use of interhole delays of 2 ms, gains of approximately 2 and 3·5% may be achieved in the P-G domain. Gains in the intermediate and fine fractions may not be significant if one is to consider the variation associated with modelling predictions.

Preliminary modelling results have highlighted the need to further quantify the potential impact of short delays on near and far field damage, as well as downstream loading productivity. This should be considered a priority if short interhole delays are to be used in primary rock production blasting.

References

1. V. M. Kuznetsov: 'The mean diameter of fragments formed by blasting rock', *Sov. Min. Sci.*, 1973, **9**, (2), 144–148.
2. C. V. Cunningham: 'The Kuz–Ram model for prediction of fragmentation from blasting', Proc. 1st Int. Symp. on 'Rock fragmentation by blasting', Luleå, Sweden, August 1983, Luleå University of Technology, 439–453.
3. C. V. Cunningham: 'Fragmentation estimations and the Kuz–Ram model – four years on', Proc. 2nd Int. Symp. on 'Rock fragmentation by blasting', Keystone, CO, USA, August 1987, Society for Experimental Mechanics, 475–487.
4. C. V. Cunningham: 'The Kuz–Ram fragmentation model – 20 years on', Proc. 3rd EFEE World Conf. on 'Explosives and blasting', Brighton UK, September 2005, EFEE, 201–210.
5. F. Ouchterlony: 'The Swebrec function: linking fragmentation by blasting and crushing', *Trans. Inst. Min. Metall. A*, 2005, **114A**, (1), A29–A44.
6. F. Ouchterlony, M. Olsson, U. Nyberg, P. Andersson and L. Gustavsson: 'Constructing the fragment size distribution of a bench blasting round, using the new Swebrec function', Proc. 8th Int. Symp. on 'Rock fragmentation in blasting', Santiago, Chile, May 2006, EDITEC S.A. Chile, 332–344.
7. D. Thornton, S. S. Kanchibotla and I. Brunton: 'Modelling the impact of rockmass and blast design variation on blast fragmentation', Proc. EXPLO 2001, Hunter Valley, NSW, Australia, October 2001, The Australian Institute of Mining and Metallurgy, 331–345.
8. I. Onederra, S. Esen, and A. Jankovic: 'Estimation of fines generated by blasting – applications for the mining and quarrying industries', *Trans. Inst. Min. Metall. A*, 2004, **113A**, (4), 237–247.
9. I. Onederra: 'A delay timing factor for empirical fragmentation models', *Trans. Inst. Min. Metall. A*, 2008, **116A**, (4), 176–179.
10. I. Onederra and K. Riihioja: 'An alternative approach to determine the uniformity index of Rosin–Rammler based fragmentation models', Proc. 8th Int. Symp. on 'Rock fragmentation in blasting', Santiago, Chile, May 2006, EDITEC S.A. Chile, 193–199.
11. I. Onederra: 'Empirical charts for the estimation of minimum response time (Tmin) in free face blasting', *Trans. Inst. Min. Metall. A*, 2007, **116A**, (1), 7–15.
12. V. Svahn: 'Generation of fines around a borehole: a laboratory study', Proc. 7th Int. Symp. on 'Rock fragmentation by blasting', Beijing, China, August 2002, Metallurgical Industry Press, 122–127.
13. I. Onederra: 'A fragmentation modelling framework for underground ring blasting applications', *Int. J. Blast. Fragment.*, 2004, **8**, (3), 177–200.
14. N. Djordjevic: 'Origin of blast induced fines', *Trans. Inst. Min. Metall.*, 2002, **111**, A143–A146.
15. S. Esen, I. Onederra, and H. Bilgin: 'Modelling the size of the crushed zone around a blasthole.', *Int. J. Rock Mech. Min. Sci.*, 2003, **40**, 485–495.
16. P. D. Katsabanis: 'Explosives technology – open pit and underground blasting', Part D, Chap. 5; 1996, Kingston, Ont., Canada, Queen's University.
17. Q. Liu and P. D. Katsabanis: 'A theoretical approach to stress waves around a borehole and their effect on rock crushing', Proc. 4th Int. Symp. on 'Rock fragmentation by blasting', Vienna, Austria, July 1993, AA Balkema, 9–16.
18. Q. Liu: 'Estimation of dynamic pressure around a fully loaded blasthole in rock', Proc. FragBlast 7: 'Rock fragmentation by blasting', Beijing, China, August 2002, Beijing Metallurgical Industry Press, 267–278.
19. J. P. Latham, J. Kemeny, N. Maerz, M. Noy, J. Schleifer and S. Tose: 'A blind comparison between results of four image analysis systems using a photo-library of piles of sieved fragments', *Int. J. Blast. Fragment.*, 2003, **7**, (2), 105–132.
20. J. A. Sanchidrian, P. Segarra and L. M. Lopez: 'A practical procedure for the measurement of fragmentation by blasting by image analysis', *Rock Mech. Rock Eng.*, 2006, **39**, (4), 359–382.